



# Journal of Population Therapeutics & Clinical Pharmacology

REVIEW ARTICLE

DOI: 10.47750/jptcp.2022.870

## A review on plant-mediated selenium nanoparticles and its applications

Jayapriya Johnson, Rajeshkumar Shanmugam\* and Thangavelu Lakshmi

Center for Transdisciplinary Research (CFTR), Nanobiomedicine Lab, Department of Pharmacology, Saveetha Dental College, Saveetha Institute of Medical and Technical Science, Saveetha University, Chennai, India

**\*Corresponding author:** RajeshkumarS, Center for Transdisciplinary Research (CFTR), Nanobiomedicine Lab, Department of Pharmacology, Saveetha Dental College, Saveetha Institute of Medical and Technical Science, Saveetha University, Chennai, India. Email: [ssrajeshkumar@hotmail.com](mailto:ssrajeshkumar@hotmail.com)

**Submitted: 28 August 2021; Accepted: 16 October 2021; Published: 6 January 2022**

---

### ABSTRACT

Nanotechnology explores a variety of promising approaches in the field of biomedical sciences. For biogenesis of selenium (Se) nanoparticles different parts of a plant are used as they contain metabolites such as alkaloids, flavonoids, phenols, proteins, and other phytochemicals which act as reducing agent to produce and stabilize nanoparticles. Nanotechnology is also widely practiced in medicine, agriculture, and many other technologies. This review is focused on green synthesis and its latest developments for the fabrication of Se nanoparticles. This research article also summarizes Se nanoparticles and different plants individually and combined along with their characterizations, using techniques such as ultraviolet–visible spectroscopy, transmission electron microscopy, and scanning electron microscopy, which specified the range, shape, size, and other specifications to easily identify and explore the studies further.

**Keywords:** *green synthesis, nanoparticles, plant extracts, selenium nanoparticles*

### INTRODUCTION

Nanotechnology is one of the most promising technologies which opens a large scope of novel applications in the area of sciences.<sup>1</sup> Eco-friendly synthesis of nanoparticles using microbes,<sup>2</sup> algae,

and plant materials is of great interest in the current research.<sup>3</sup> Plants used for synthesizing nanoparticles are *Vitis vinifera*,<sup>4</sup> *Cissus quadrangularis*,<sup>5</sup> *Piper nigrum*,<sup>6</sup> *Garcinia mangostana*,<sup>7</sup> *Nitraria schoberi*,<sup>8</sup> *Abelmoschus esculentus*,<sup>9</sup> *Medicago*

J Popul Ther Clin Pharmacol Vol 28(2):e29–e40; 6 January 2022.

This article is distributed under the terms of the Creative Commons Attribution-Non Commercial 4.0 International License. ©2022 Rajeshkumar S et al.

*sativa*,<sup>10</sup> *Andrographis paniculata*,<sup>11</sup> turmeric,<sup>12</sup> green apple,<sup>13</sup> lemon grass,<sup>14</sup> red apple,<sup>15</sup> black tea,<sup>16</sup> and green tea.<sup>17</sup> Green synthesis of nanoparticles using plant materials through well-known phytochemical metal nanoparticles has been used in cancer therapy, targeted drug delivery, molecular imaging, waste water treatment, catalysis, biosensor development, fuel elements, cosmetics and antiseptics.<sup>17-19</sup> The word “selenium” originates from the Greek word “Selene” which means moon goddess.<sup>20</sup> Selenium (Se) has unique properties and great potential in the field of physics, chemistry, and biology.<sup>21</sup> It is a trace element found in both plants and mammals.<sup>22</sup> The deficiency of Se is associated with disease in man; it is effective against different types of cancer and neurodegenerative diseases.<sup>23-26</sup> Se prepared through biological way, from plants such as *V.vinifera*,<sup>27</sup> *Capsicum annum*,<sup>25</sup> garlic,<sup>26-28</sup> and

fenugreek, is less toxic than that prepared through chemical synthesis. In some research articles, it has been shown that it is active against human breast cancer cells to make nanotubes<sup>29</sup> and nanowires, and to prevent DNA damage.<sup>30</sup>

## PLANT-MEDIATED NANOPARTICLES

### *Vitis vinifera*

Sharma et al. have reported an eco-friendly method for fabrication of very small and uniform Se nano balls. This biological approach focused on biosynthesis of selenium nanoparticles (SeNPs) using dried *V. vinifera* extract. The initial confirmation was made by the color change of solution from colorless to brick red color. Transmission electron microscopy (TEM) images confirmed their morphology and size to be spherical and 3–18 nm



FIGURE 1. Different plants used in selenium nanoparticles synthesis.

diameter in size. The zeta average diameter measured  $8.12 \pm 2.5$  nm, width 0.212 PDI (polydispersity index). The crystalline nature of SeNPs was confirmed by the X-ray diffraction (XRD) study. Fourier transform infrared (FTIR) analysis results on sharp absorption fix at  $3420\text{ cm}^{-1}$  assigned to OH and  $1620\text{ cm}^{-1}$  corresponded to the C-H vibration of the aromatic ring. The result indicated the presence of lignin (a phenolic compound), a biopolymeric agent which may be responsible for both reduction and stabilization of the Se nano balls.<sup>26</sup>

### *Allium sativum*

Anu et al. fabricated SeNPs using garlic clove extract. They stated that by adding garlic extract, it reduced selenite into Se and showed colorchange where it was initially colorless and then became brick red after 5 days of incubation. The spectral measurement ranged about 200–700 nm, and the maximum absorption was exhibited at 260 nm. The results of TEM analysis revealed the morphology of SeNPs generated from garlic cloves; their size ranged from 40 to 100 nm, they were spherical and mono dispersed in nature. Scanning electron microscopy (SEM) images indicated deposition of SeNPs. EDX pattern pointed to strong signal of Se. The XRD analysis showed prominent peaks. These patterns described the amorphous nature of Se particles. In garlic extract, FTIR analysis results indicated the presence of NO nitro group and CO carboxyl group. The cytotoxicity investigation proved that MTT assay of vero cells treated chemically led to  $CC_{50}$  of  $18.8 \pm 0.8\text{ }\mu\text{g/mL}$ , with green synthesized produced  $CC_{50}$  of  $31.8 \pm 0.6\text{ }\mu\text{g/mL}$ .<sup>28</sup>

Satgurunathan et al. approached on an eco-friendly method using garlic clove. It was found as an effective reducing and stabilizing agent, which also turned colorless solution to brown. Synthesis of SeNPs was achieved by addition of garlic clove extract. In ultraviolet–visible (UV-Vis) spectroscopy, the absorbance was detected at 267–367 nm. In SEM analysis, the synthesized SeNPs were found to be spherical in shape with size 48–87 nm.

Energy dispersive X-ray analysis (EDX) spectrum confirmed elemental composition of SeNPs which indicated the presence of 80% Se. The XRD patterns suggested that the sample is nanocrystalline in nature, which matched very well with standard Se powder and confirmed the formation of SeNPs. FTIR analysis results indicated that C-H, C=O, NO nitro group, and CO carboxyl group in garlic extract were involved in the reduction of sodium selenite to SeNPs. The green synthesis of SeNPs has improved the survival, growth X, and concentration of biochemical constituents in *Macrobrachium rosenbergii* PL when fed through the life feed Artemianauplii ( $P < 0.05$ ). Furthermore,  $101.04\text{ }\mu\text{g/L}$  of SeNPs was found to be nontoxic to *M. rosenbergii* PL when fed with 1-hour enriched Artemianauplii, as the insignificant ( $P > 0.05$ ) alternation activities of superoxides, dismutase, and catalase were recorded. These facts suggested that  $101.04\text{ }\mu\text{g/L}$  of SeNPs was the optimized concentration to enrich Artemia nauplii for 0.5–1 h duration. It was concluded that the same principle can be adopted for feeding the larvae of any finfish or shellfish when supplementing trace elements.<sup>31</sup>

Babu et al. in 2016 green synthesized nanoparticles from *Allium sativum*. The color change was monitored. The change from yellowish orange to red was related to the increase in concentration of plant extract, which indicated the surface plasmon vibrations of SeNPs. The formation of SeNPs was confirmed by UV-Vis spectroscopy, the absorbance was between 200 and 300 nm regions. The SEM images scrutinized the morphology of SeNPs and were confirmed as spherical in shape. The FTIR studies confirmed the peaks at  $3446.2\text{ cm}^{-1}$  carboxylic OH stretching to shift to  $3298.7\text{ cm}^{-1}$  assigned for stretching of O-H, N-H amide group which was responsible for the formation of SeNPs. The Raman spectroscopy microscopic images have shown the characteristic feature of Se in the form of ruby red color. In XRD analyses, the size of crystalline nanoparticles was found to be 24.57 nm, which clearly indicated the amorphous nature of Se, and represented red

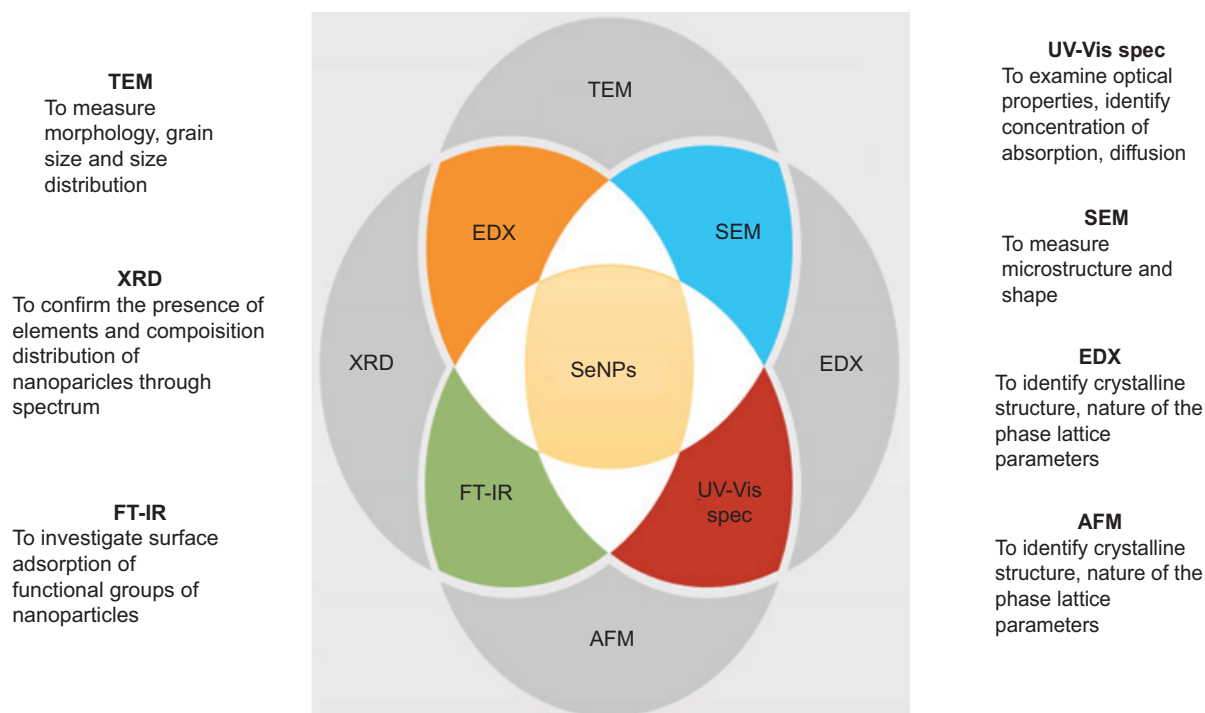


**FIGURE 2.** Characterization of SeNPs using various techniques.

color. This technique was employed to understand the electrochemical properties of increased concentration of CT-DNA-SeNPs complex in TAE buffer at room temperature with a potential ranged from  $-1.5$  V to  $0$  V. It also indicated that on addition of increasing concentration of CT-DNA-SeNPs complex, both anodic peak potential (Epa) and cathodic peak potential (Epc) showed positive shifts. These findings clearly indicated that the shifts in CV potentials are due to interpose of molecules into DNA helix. This study concluded that the SeNPs bound to DNA via interaction by intersection of SeNPs between the base pairs of DNA helix.<sup>28</sup>

### *Petroselinum crispum*

Fritea et al. for the first time explored the green synthesis of SeNPs from parsley leaves aqueous extract at room temperature. The characterization techniques used were UV-Vis, FTIR, atomic force microscopy (AFM), and dynamic light scattering

(DLS). In UV-Vis spectroscopy, the range was recorded at  $200$ – $800$  nm. The extract was confirmed by colorchange from light brown to orange and then to red. In DLS, measurement of parsley extract indicated two maximum distributions. The maximum distribution was around  $400$  nm. AFM images were recorded from a limited area of a dried film of SeNPs. The apparent zeta potential was recorded at a maximum value of  $-14.2$  mV. In the FTIR, the high wavelength range was at  $3280$   $\text{cm}^{-1}$  due to OH stretching of the aromatic rings and a sharp peak at  $2918$   $\text{cm}^{-1}$ , which represented ether-methoxy ( $\text{OCH}_3$ ) groups.<sup>32</sup>

### *Lycium barbarum*

Zhang et al. scrutinized the morphological and structural features of synthesized Lyciumbarbarum polysaccharides green tea SeNPs (LBP-GT-SeNPs). TEM images confirmed nanoscale-ranged spherical and triangular shape; EDX spotted dark dots in

small area. The typical XRD pattern revealed the polymorph, while the prepared nano Se was amorphous. In FTIR spectra analysis confirmed the presence of LBP on the surface SeNPs. The stretching vibration peak of hydroxide was blue-shifted from  $3392\text{ cm}^{-1}$  to  $3377\text{ cm}^{-1}$ , suggesting that Se interacted with hydroxyl group from LBP through LBP-GT-SeNPs which were spherical in shape and stable. The functionalized nanoparticles demonstrated high 2,2-diphenyl-1-picrylhydrazyl (DPPH) scavenging ability and 2,2'-azino-bis(3-ethylbenzothiazoline-6-sulfonic acid) (ABTS) scavenging ability. LBP-GT-SeNPs against oxidative stress-induced cell death was investigated by MTT assay. LBP-GT-SeNPs protected PC12 against  $\text{H}_2\text{O}_2$ -induced toxicity. The cells introduced to LBP-GT-SeNPs treated with  $\text{H}_2\text{O}_2$  exhibited 90% viability. The result suggested that SeNPs have the potential for utilization as food materials in green synthesis of SeNPs.<sup>33</sup>

#### ***Diospyros montana***

Kokila et al. worked on phytochemical analysis of *Diospyros montana* leaf aqueous extract. It was an effective capping agent because it contained flavonoids, phenols, carbohydrate, protein, saponins, terpenoids, glycosides, and tannins. Phenols and flavonoids acted as reducing agents. The antioxidant activity data confirmed the dependency on particle size and concentration. The  $\text{IC}_{50}$  value of the nanoparticle was  $0.225\text{ mg/mL}$ . When compared to standard ascorbic acid, the  $\text{IC}_{50}$  value  $0.138$  was  $\text{mg/mL}$ . The antimicrobial activity was investigated against pathogenic microorganisms using disc diffusion method. The zone of inhibition was found highest for *Aspergillus niger* (12 mm) when compared to *Staphylococcus aureus* (8 mm) and *Escherichia coli* (7 mm). Cytotoxic properties indicated 15% of cell death ( $\text{IC}_{50}$ ) in MCF-7 cell lines treated with SeNPs, which was  $80.83\text{ mg/mL}$ . Also, green synthesis of SeNPs enhanced cytotoxicity when compared to chemical-based synthetic drugs. These nano-sized SeNPs can be potentially used as effective pharmacological agents in food industries.<sup>34</sup>

#### ***Clausenadentata***

Sowndarya et al. stated that SeNPs derived from *Clausena dentate* leaf extracts via green synthesis exhibited strong mosquito larvicidal activity in a dose-dependent manner. The synthesis of SeNPs was confirmed by UV spectrometry through color change from black to yellow at 420 nm. In FTIR spectroscopy, the band was present at  $2922.25\text{ cm}^{-1}$  N-H group. This was also mentioned in EDX analysis which gave further insight on SeNPs. The peak at  $72.64\text{ cm}^{-1}$  confirmed the binding intensity of Se. In SEM analysis, the synthesized Se was spherical and uniformly distributed, the size ranged from 46.32 to 78.88 nm. The synthesized Se showed high mortality at very low concentrations.  $\text{LC}_{50}$  values were  $240.74\text{ mg/L}$ ,  $104.13\text{ mg/L}$ , and  $99.602\text{ mg/L}$  against mosquito larvae of *Anopheles stephensi*, *Aedes aegypti*, *Culex quinquefasciatus*, respectively.<sup>35</sup>

#### ***Hawthorn fruit***

SeNPs were synthesized by Cui et al. using aqueous hawthorn fruit extract (HE). Firstly, they confirmed the presence of Se by visual observation, which turned brown color. Further TEM photographs indicated uniform spherical HE-SeNPs. The size and zeta potential of SeNPs were 113 nm, and both HE and HE-SeNPs solutions exhibited absorption at 2010 nm and 2080 nm, respectively. Regarding cytotoxic activity, the aqueous extract of HE-SeNPs in HepG2 cells was evaluated through MTT assay which depicted that HE had unobtrusive proliferative inhibition effect in HepG2 cells at concentrations 5, 10, 20, and 40  $\text{mg/mL}$ . However, it showed antitumor activity toward HepG2 cells with an  $\text{IC}_{50}$  of  $1.922 \pm 5.3\text{ mg/mL}$ . The flow cytometry results revealed that both early and total apoptosis rates increased after treating with HE-SeNPs in HepG2 cells. They also measured the reactive oxygen species (ROS) of HepG2 cells after treatment with HE-SeNPs. The treatment with HE-SeNPs elevated intracellular ROS, which suggested that the apoptosis was induced by the

He-SeNPs, was related to the generation of intracellular ROS. The shift fluorescence from red to green indicated the rapid decrease in mitochondrial membrane potential (MMP) after treatment with HE-SeNPs. Thus, HE-SeNPs induced the increase of dose-dependent caspase -9 levels and decreased BCL-2 levels.<sup>36</sup>

### ***Emblica officinalis***

In the research by Gunti et al., phytofabricated SeNPs from aqueous fruit extract of *Emblica officinalis* were found to be rich in phenolics ( $59.18 \pm 2.91$  mg GAE/g), flavonoids ( $38.50 \pm 2.84$  mg CE/g), and tannins ( $44.28 \pm 3.09$  mg TAE/g). The characterization of PF-SeNPs was confirmed by the color change into brick red when fruit extract was added after 24 h. The results were also confirmed by FTIR peaks and UV spec absorption observed at 270 nm. The sharp peak of zeta potential for PF-SeNPs was noticed at  $-24.4$  mV, and it was negatively charged ion. Further, the DLS pattern revealed optimized SeNPs, the sizes ranged from 20 to 60 nm which showed that the nanoparticles were monodispersed. The spherical morphology of SeNPs was confirmed by SEM analysis. EDX spectrum confirmed the presence of elemental Se (61.60%), C (29.96%), and O (4.41%). The shape and size were confirmed by HR-TEM analysis, the average diameter being 15–40 nm. Antioxidant activity for PF-SeNPs was determined as  $15.67 \pm 1.41$  and  $18.84 \pm 1.02$   $\mu\text{g/mL}$  for DPPH, and  $\text{EC}_{50}$  values of ascorbic acid was noted as  $19.21 \pm 2.63$  and  $21.69 \pm 1.77$   $\mu\text{g/mL}$  for DPPH and ABTs radical scavenging activity, respectively. The PF-SeNPs also showed minimum and maximum inhibitory concentrations against both gram-positive and gram-negative bacteria, with the most effectivity on fungi pathogens. In this research, they finally concluded with biocompatibility assay where PF-SeNPs were assessed in N2a cells with  $\text{IC}_{50}$  value compared to sodium selenite. In addition, MMP and caspase-3 PF-SeNPs were less toxic and much safer. Therefore, this study has clearly stated that PF-SeNPs have tremendous

applications in biomedical, food, and pharmaceutical industries, and they are potential antimicrobial and antioxidant agents.<sup>37</sup>

### ***Peltophorum pterocarpum***

Ganesan et al. reported a novel technology for the synthesis of SeNPs using the flowers of *Catharanthus roseus* and *Peltophorum pterocarpum*. The visual observation of *C. roseus* indicated pale green turned to pinkish red due to reducing activity, while in *P. pterocarpum*, transparent orange turned light brown. In UV-Vis spectroscopy analysis, the surface plasmon resonance (SPR) vibration ranged at 335 nm for *C. roseus* and 325 nm for *P. pterocarpum*, respectively. The major peak of *C. roseus*-mediated reaction medium (0.751) was found elevated than the reaction medium (0.588) prepared with *P. pterocarpum*. The single peak in the SPR band indicated that the synthesized nanoparticles were spherical. Luminescence spectroscopic analysis confirmed the formation of SeNPs. The exhibition spectrum recorded  $\lambda_{\text{max}}$  364.5 nm for *C. roseus* and 364 nm for *P. pterocarpum*. FTIR analysis revealed that the functional groups such as esters, and secondary and tertiary amides derived from the flower of *C. roseus*,  $1736$   $\text{cm}^{-1}$ , depleted sodium selenate with the help of ketones and primary amides, while in *P. pterocarpum*, vital absorbance band was slightly higher at  $1775$   $\text{cm}^{-1}$ . The XRD studies confirmed the formation of FCC (face-centered cubic) phase of SeNPs, with an average size of 32.02 nm and 40.2 nm with flower broths of *C. roseus* and *P. pterocarpum*, respectively. The EDX and SEM studies confirmed the formation of elemental spherical SeNPs. Further TEM analysis predicted the morphology and size of the nanoparticles from the flower broths of *C. roseus* and *P. pterocarpum*, which formed hollow spherical SeNPs with an average size of  $23.2 \pm 6.06$  nm and  $30.44 \pm 2.89$  nm, respectively. This study proved that this bioinspired way was a facile, environmentally benign, and green alternate route to physical and chemical methods.<sup>40</sup>

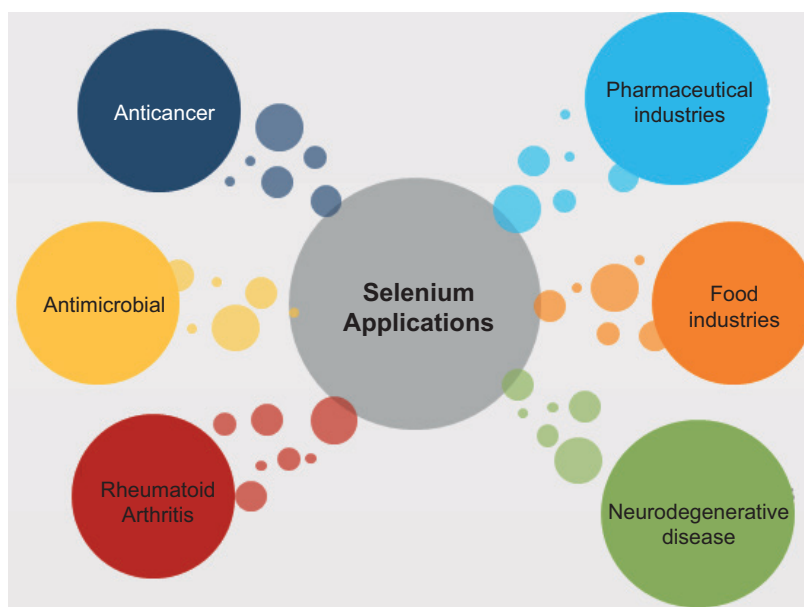


**FIGURE 3.** Biomedical applications of SeNPs.

#### *Withania somnifera*

Alagasan et al. synthesized SeNPs using *Withania somnifera* leaves extract which possessed active constituents such as alkaloids, flavonoids, phenolics, tannins, and terpenoids, which acted as good reducing agents for the preparation of SeNPs. The color changed from colorless to ruby red color. UV-VIS spectroscopy was used to examine the formation of SeNPs which showed at 320 nm. The FTIR analysis indicated the presence of various functional groups. A broad peak absorbed at  $3434\text{ cm}^{-1}$  corresponded to the O-H stretch in alcohols and phenols. The sharp peaks noted at  $1375\text{ cm}^{-1}$  was attributed to the C-H bending alkanes. XRD analysis revealed that SeNPs are amorphous in nature, crystalline sized 15 nm. The FE-SEM image of SeNPs revealed that diameter ranged from 45 to 90 nm. EDX identified Se as intense, with narrow width and high purity. The TEM analysis revealed the amorphous nature of SeNPs. Green synthesized SeNPs were found to possess significant antioxidant activity ( $\text{IC}_{50}$  14.81  $\mu\text{g}/\text{mg}$ ) and acted as a potential antibacterial agent on *Bacillus subtilis* (12 mm), *Klebsiella pneumoniae* (14 mm), and

*S. aureus* (19.66 mm). The antiproliferative activity result suggested that SeNPs possess higher growth control against A549 lung carcinoma cancer cells ( $\text{IC}_{50}$  at 25  $\mu\text{g}/\text{mL}$ ) which indicated their potential in medical applications. The photocatalytic study concluded that these SeNPs have efficiency to degrade methylene blue under sunlight irradiation. Hence, this can be applied in water treatment plants and textile industries and serves an efficient role in multifaceted pharmacological properties.<sup>39</sup>

#### Fenugreek

A study by Ramamurthy et al. in 2019 showed the presence of alkaloids, flavonoids, amino acids, protein, carbohydrate, cardiac glycosides, and saponins in aqueous extract of fenugreek seeds. SeNPs were characterized by UV-Vis spectrophotometer, the absorbance was noted at 200–400 nm, and it changed from colorless to ruby red color. The SEM and FTIR analysis showed vibrational bond bending and stretching of functional groups which indicated the presence of reducing group responsible for the reduction of SeNPs. The XRD pattern suggested that the sample was nanocrystalline in nature. The

significant MCF-7 cancer cells were observed at 6 h and 36 h in 100 µg/mL and 25 µg/mL, respectively. The combination of SeNPs with doxorubicin, the so-called conjugated nanocomposites, provided good anticancer effect when compared to individual ones. The results also revealed that SeNPs induced MCF-7 cell death through apoptosis.<sup>40</sup>

### *Aloe vera*

A study by Fardsadegh et al. in 2019 using *Aloe vera* leaf extract (ALE) fabricated with SeNPs indicated three centered main peaks at 572.8 cm<sup>-1</sup>, 1635.52 cm<sup>-1</sup>, and 3454.3 cm<sup>-1</sup>. In that, 1635.52 cm<sup>-1</sup> was attributed to amide I group, which was related to proteins and had a key role in the stabilizing of formed SeNPs. Regression coefficients R<sup>2</sup> and R<sup>2</sup>-adj had higher values (>94.00). Furthermore, it was observed that insignificant (P>0.05) number of their generated models showed appropriate fitness to their synthesis variables. Additionally, quadratic term of the amount of Na<sub>2</sub>SeO<sub>3</sub> solution and its interaction with the amount of ALE solution had inconsequential effects on the color intensity which formed SeNPs. The color intensity increased with increase in amount of Se ions in the solution. The repulsion of the system increased due to positive charge of the ions, and rate of nucleation decreased the maximum color intensity (2.99 % a.u), which was obtained by using 4.41 mL of ALE and 12.93 mL of Na<sub>2</sub>SeO<sub>3</sub> solution. According to an overlaid counter plot of fabricated SeNPs, using 4.92 mL of ALE and 13.03 mL of Na<sub>2</sub>SeO<sub>3</sub> obtained the color intensity and particle size of 3.0% a.u. and 33.30 nm, respectively, which were analysed through TEM. It was also revealed that there were inconsequential effects between the predicted and expression values. In UV spectrophotometry analysis, λ<sub>max</sub> was achieved at 323 nm, centered between 295 and 340 nm. DLS analysis using *Aloevera* indicated that spherical fabricated SeNPs with mean particle size, PDI, and zeta potential values of 50 nm, 0.344, and -18 mV, respectively, were obtained using optimum synthesis conditions of 13.03 mL of Na<sub>2</sub>SeO<sub>3</sub> and 4.92 mL of ALE. On

analysis of the antibacterial activity, in diameter, the zone of inhibition observed for *S. aureus* (12 mm) was higher than *E.coli* (10 mm). Further, the analysis of the antifungal activity on mycelia growth of *Penicillium digitatum* and *Colletotrichum coccodes*, incubated for 7 days at 26 ± 2°C, revealed that *P. digitatum* inhibited mycelia growth, while low fungicidal effect was observed in *C. coccodes*.<sup>41</sup>

### **Ginger**

Menon et al. practiced biological methods for synthesis of SeNPs from *Zingiberofficinale*. Firstly, they observed visual results by confirming the color change from pale yellow to red. In UV analysis, the peak was noted between 370 and 420 nm after 74 h incubation. The nanoparticles obtained a spherical shape, with sizes ranging from 100 to 150 nm. EDX spectrum confirmed the presence of Se, it was a 1.37 keV absorption signal. In FTIR, aromatic compounds such as flavonoids and terpenoids were present. The particle size, distribution porosity, surface roughness, and morphology were depicted through AFM; the white spots were believed to be SeNPs in SEM and TEM results. The zeta potential of SeNP was found to be at -36 mV. For SeNP, the measurement of size distribution and purity was within 100–120 nm, measured by DLS. The antibacterial activity results revealed Se as a potential candidate against *E.coli*, *Proteus sp*, *Serratia sp*, and *Klebsiella*. *Proteus* gave the highest zone of inhibition. The antioxidant activity and the ascorbic acid value was recorded at 250 µg/mL. The results stated that SeNPs are free radical inhibitors which were involved in the bioreduction and capping of the SeNPs.<sup>42</sup>

### *Pelargonium zonale*

Fardsadegh et al. focused on the biogenic synthesis of SeNPs using *Pelargonium zonale* leaf extract (PLE) under microwave irradiation. The PLE specification was highlighted at two main peaks, at 3452.5 cm<sup>-1</sup> and 1636.5 cm<sup>-1</sup>, related to the stretching vibration of hydroxyl and amide groups

which played a key role in Se. The SPR signal wavelength of SeNPs ranged from 270 to 350 nm. The color changed from pale yellow to dark red. The particle size and zeta potential values were recorded using DLS analyser. The TEM images achieved optimum conditions and revealed a spherical shape. The particle sized ranged from 40 to 60 nm. The zeta potential was  $-24.6$  mV, absorbance unit was 34.6%, and the broad absorption peak was recorded at 319 nm, formed at optimum conditions with 1.48 mL and 15 mL of PLE and sodium selenite solutions, respectively. The antibacterial activity of these SeNPs against *S. aureus* (10 mm) was higher than *E. coli* (9 mm). These results indicated that PLE and  $\text{Na}_2\text{SeO}_3$  solution had no bacteriostatic activity toward bacterial strains. The fabricated SeNPs had PLE on mycelial growth of *P. digitatum* and *C. coccodes*. It clearly stated that *P. digitatum* had higher antifungal activity than *C. coccodes*. This was a clean, fast, cost-effective, and one-step synthesis process for the synthesis of other metal and metal oxide nanoparticles.<sup>41</sup>

## CONCLUSION

In summary, the property of SeNPs is not limited to biological applications. Nature has excellent and inventive methods for making the most competent miniaturized functional materials. The synthesis of SeNPs from plant extract is economical, energy efficient, and cost-effective. Only few reports have been published about the synthesis of SeNPs. There is still a need to explore the green synthesis method of SeNPs to uplift and overcome many medical and therapeutic conditions. SeNPs have emerged in present and future era, with a variety of applications incorporating food, textile, and pharmaceutical industries.

## REFERENCES

1. Kargozar S, Mozafari M. Nanotechnology and nanomedicine: Start small, think big. Mater

- Today Proc. 2018;5(7):15492–500. <https://doi.org/10.1016/j.matpr.2018.04.155>
2. Malarkodi C, Rajeshkumar S, Vanaja M, Paulkumar K, Gnanajobitha G, Annadurai G. Eco-friendly synthesis and characterization of gold nanoparticles using *Klebsiellapneumoniae*. J Nanostructure Chem. 2013;3(1):30. <https://doi.org/10.1186/2193-8865-3-30>
3. Ramakrishna M, Babu DR, Gengan RM, Chandra S, Rao GN. Green synthesis of gold nanoparticles using marine algae and evaluation of their catalytic activity. J Nanostructure Chem. 2016;6(1):1–3. <https://doi.org/10.1007/s40097-015-0173-y>
4. Gnanajobitha G, Paulkumar K, Vanaja M, Rajeshkumar S, Malarkodi C, Annadurai G, et al. Fruit-mediated synthesis of silver nanoparticles using *Vitisvinifera* and evaluation of their antimicrobial efficacy. J Nanostructure Chem. 2013;3(1):67. <https://doi.org/10.1186/2193-8865-3-67>
5. Vanaja M, Gnanajobitha G, Paulkumar K, Rajeshkumar S, Malarkodi C, Annadurai G. Phytosynthesis of silver nanoparticles by *Cissusquadrangularis*: Influence of physicochemical factors. J Nanostructure Chem. 2013;3(1):17. <https://doi.org/10.1186/2193-8865-3-17>
6. Paulkumar K, Gnanajobitha G, Vanaja M, Rajeshkumar S, Malarkodi C, Pandian K, et al. Piper nigrum leaf and stem assisted green synthesis of silver nanoparticles and evaluation of its antibacterial activity against agricultural plant pathogens. Sci World J. 2014;2014:829894. <https://doi.org/10.1155/2014/829894>
7. Karthiga P, Rajeshkumar S, Annadurai G. Mechanism of larvicidal activity of antimicrobial silver nanoparticles synthesized using *garciniamangostana* bark extract. J Cluster Sci. 2018;29(6):1233–41. <https://doi.org/10.1007/s10876-018-1441-z>
8. Santhoshkumar J, Rajeshkumar S, Kumar SV. Phyto-assisted synthesis, characterization and applications of gold nanoparticles—A review. Biochem Biophys Rep. 2017;11:46–57. <https://doi.org/10.1016/j.bbrep.2017.06.004>
9. Mollick MM, Rana D, Dash SK, Chattopadhyay S, Bhowmick B, Maity D, et al. Studies on

- green synthesized silver nanoparticles using *Abelmoschus esculentus* (L.) pulp extract having anticancer (in vitro) and antimicrobial applications. *Arab J Chem*. 2019;12(8):2572–84. <https://doi.org/10.1016/j.arabjc.2015.04.033>
10. Marchiol L, Mattiello A, Pošćić F, Giordano C, Musetti R. In vivo synthesis of nanomaterials in plants: Location of silver nanoparticles and plant metabolism. *Nanoscale Res Lett*. 2014;9(1):101. <https://doi.org/10.1186/1556-276X-9-101>
  11. Rajakumar G, Thiruvengadam M, Mydhili G, Gomathi T, Chung IM. Green approach for synthesis of zinc oxide nanoparticles from *Andrographis paniculata* leaf extract and evaluation of their antioxidant, anti-diabetic, and anti-inflammatory activities. *Bioprocess Biosyst Eng*. 2018;41(1):21–30. <https://doi.org/10.1007/s00449-017-1840-9>
  12. Alsammarraie FK, Wang W, Zhou P, Mustapha A, Lin M. Green synthesis of silver nanoparticles using turmeric extracts and investigation of their antibacterial activities. *Colloids Surf B Biointerfaces*. 2018;171:398–405. <https://doi.org/10.1016/j.colsurfb.2018.07.059>
  13. Rajeshkumar S, Bharath LV. Mechanism of plant-mediated synthesis of silver nanoparticles—A review on biomolecules involved, characterisation and antibacterial activity. *Chem Biol Interact*. 2017;273:219–27. <https://doi.org/10.1016/j.cbi.2017.06.019>
  14. Agarwal H, Kumar SV, Rajeshkumar S. Antidiabetic effect of silver nanoparticles synthesized using lemongrass (*Cymbopogon citratus*) through conventional heating and microwave irradiation approach. *J Microbiol Biotechnol Food Sci*. 2020;9(6):371–6. <https://doi.org/10.15414/jmbfs.2018.7.4.371-376>
  15. Umoren SA, Obot IB, Gasem ZM. Green synthesis and characterization of silver nanoparticles using red apple (*Malus domestica*) fruit extract at room temperature. *J Mater Environ Sci*. 2014;5(3):907–14.
  16. Lebaschi S, Hekmati M, Veisi H. Green synthesis of palladium nanoparticles mediated by black tea leaves (*Camellia sinensis*) extract: Catalytic activity in the reduction of 4-nitrophenol and Suzuki–Miyaura coupling reaction under ligand-free conditions. *J Colloid Interface Sci*. 2017;485:223–31. <https://doi.org/10.1016/j.jcis.2016.09.027>
  17. Selvan DA, Mahendiran D, Kumar RS, Rahiman AK. Garlic, green tea and turmeric extracts-mediated green synthesis of silver nanoparticles: Phytochemical, antioxidant and in vitro cytotoxicity studies. *J Photochem Photobiol B*. 2018;180:243–52. <https://doi.org/10.1016/j.jphotobiol.2018.02.014>
  18. Khan ZU, Khan A, Chen Y, Shah NS, Muhammad N, Khan AU, et al. Biomedical applications of green synthesized noble metal nanoparticles. *J Photochem Photobiology B*. 2017;173:150–64. <https://doi.org/10.1016/j.jphotobiol.2017.05.034>
  19. Singh J, Dutta T, Kim KH, Rawat M, Samddar P, Kumar P. “Green” synthesis of metals and their oxide nanoparticles: Applications for environmental remediation. *J Nanobiotechnol*. 2018;16(1):84. <https://doi.org/10.1186/s12951-018-0408-4>
  20. Chhabria S, Desai K. Selenium nanoparticles and their applications. *Encyclopedia Nanosci Nanotechnol*. 2016;20:1–32.
  21. Skalickova S, Milosavljevic V, Cihalova K, Horky P, Richtera L, Adam V. Selenium nanoparticles as a nutritional supplement. *Nutrition*. 2017;33:83–90. <https://doi.org/10.1016/j.nut.2016.05.001>
  22. Schomburg L, Arnér ES. Selenium metabolism in herbivores and higher trophic levels including mammals. In: Pilon-Smits EAH, Winkel LHE, Lin ZQ, editors. *Selenium in plants*. Cham: Springer;2017. p. 123–39. [https://doi.org/10.1007/978-3-319-56249-0\\_8](https://doi.org/10.1007/978-3-319-56249-0_8)
  23. Rayman MP. Selenium and human health. *Lancet*. 2012;379(9822):1256–68. [https://doi.org/10.1016/S0140-6736\(11\)61452-9](https://doi.org/10.1016/S0140-6736(11)61452-9)
  24. Santos I, Ramos C, Mendes C, Sequeira CO, Tomé CS, Fernandes DG, et al. Targeting glutathione and cystathionine  $\beta$ -synthase in ovarian cancer treatment by selenium–chrysin polyurea dendrimer Nanoformulation. *Nutrients*. 2019;11(10):2523. <https://doi.org/10.3390/nu11102523>
  25. Rajeshkumar S, Ganesh L, Santhoshkumar J. Selenium nanoparticles as therapeutic agents

- inneurodegenerative diseases. Cham: Springer; 2019. Nanobiotechnology in neurodegenerative diseases; p. 209–24. [https://doi.org/10.1007/978-3-030-30930-5\\_8](https://doi.org/10.1007/978-3-030-30930-5_8)
26. Sharma G, Sharma AR, Bhavesh R, Park J, Ganbold B, Nam JS, et al. Biomolecule-mediated synthesis of selenium nanoparticles using dried *Vitisvinifera* (raisin) extract. *Molecules*. 2014; 19(3):2761–70. <https://doi.org/10.3390/molecules19032761>
  27. Husen A, Siddiqi KS. Plants and microbes assisted selenium nanoparticles: Characterization and application. *J Nanobiotechnol*. 2014;12(1):28. <https://doi.org/10.1186/s12951-014-0028-6>
  28. Anu K, Singaravelu G, Murugan K, Benelli G. Green-synthesis of selenium nanoparticles using garlic cloves (*Allium sativum*): Biophysical characterization and cytotoxicity on vero cells. *J Cluster Sci*. 2017;28(1):551–63. <https://doi.org/10.1007/s10876-016-1123-7>
  29. Ezhuthupurakkal PB, Polaki LR, Suyavaran A, Subastri A, Sujatha V, Thirunavukkarasu C. Selenium nanoparticles synthesized in aqueous extract of *Allium sativum* perturbs the structural integrity of calf thymus DNA through intercalation and groove binding. *Mater Sci Eng C*. 2017;74:597–608. <https://doi.org/10.1016/j.msec.2017.02.003>
  30. Menon S, KS SD, Santhiya R, Rajeshkumar S, Kumar V. Selenium nanoparticles: A potent chemotherapeutic agent and an elucidation of its mechanism. *Colloids Surf B Biointerfaces*. 2018;170:280–92. <https://doi.org/10.1016/j.colsurfb.2018.06.006>
  31. Satgurunathan T, Bhavan PS, Komathi S. Green synthesis of selenium nanoparticles from sodium selenite using garlic extract and its enrichment on *Artemianaulpii* to feed the freshwater prawn *Macrobrachiumrosenbergii* post-larvae. *Res J Chem Environ*. 2017 Oct;21:1–2.
  32. Fritea L, Laslo V, Cavalu S, Costea T, Vicas SI. Green biosynthesis of selenium nanoparticles using parsley (*Petroselinumcrispum*) leaves extract. *Studia Universitatis “VasileGoldis” Arad. Seria Stiintele Vietii (Life Sciences Series)*. 2017;27(3):203–8.
  33. Zhang W, Zhang J, Ding D, Zhang L, Muehlmann LA, Deng SE, et al. Synthesis and antioxidant properties of *Lyciumbarbarum* polysaccharides capped selenium nanoparticles using tea extract. *Artif Cells Nanomed Biotechnol*. 2018;46(7):1463–70. <https://doi.org/10.1080/21691401.2017.1373657>
  34. Kokila K, Elavarasan N, Sujatha V. *Diospyrosmontana* leaf extract-mediated synthesis of selenium nanoparticles and their biological applications. *New J Chem*. 2017;41(15):7481–90. <https://doi.org/10.1039/C7NJ01124E>
  35. Sowndarya P, Ramkumar G, Shivakumar MS. Green synthesis of selenium nanoparticles conjugated *Clausenadentata* plant leaf extract and their insecticidal potential against mosquito vectors. *Artif Cells Nanomed Biotechnol*. 2017;45(8):1490–5. <https://doi.org/10.1080/21691401.2016.1252383>
  36. Cui D, Liang T, Sun L, Meng L, Yang C, Wang L, et al. Green synthesis of selenium nanoparticles with extract of hawthorn fruit induced HepG2 cells apoptosis. *Pharm Biol*. 2018;56(1):528–34. <https://doi.org/10.1080/13880209.2018.1510974>
  37. Gunti L, Dass RS, Kalagatur NK. Phytofabrication of selenium nanoparticles from *Embllicaofficinalis* fruit extract and exploring its biopotential applications: Antioxidant, antimicrobial, and biocompatibility. *Front Microbiol*. 2019;10:931. <https://doi.org/10.3389/fmicb.2019.00931>
  38. Babajani A, Iranbakhsh A, Ardebili ZO, Eslami B. Differential growth, nutrition, physiology, and gene expression in *Melissa officinalis* mediated by zinc oxide and elemental selenium nanoparticles. *Environ Sci Pollut Res*. 2019;26(24):24430–44. <https://doi.org/10.1007/s11356-019-05676-z>
  39. Alagesan V, Venugopal S. Green synthesis of selenium nanoparticle using leaves extract of *Withaniasomnifera* and its biological applications and photocatalytic activities. *Bionanoscience*. 2019;9(1):105–16. <https://doi.org/10.1007/s12668-018-0566-8>
  40. Ramamurthy CH, Sampath KS, Arunkumar P, Kumar MS, Sujatha V, Premkumar K, et al. Green synthesis and characterization of selenium nanoparticles and its augmented cytotoxicity with doxorubicin on cancer cells. *Bioprocess BiosystEng*. 2013;36(8):1131–9. <https://doi.org/10.1007/s00449-012-0867-1>

41. Fardsadegh B, Vaghari H, Mohammad-Jafari R, Najian Y, Jafarizadeh-Malmiri H. Biosynthesis, characterization and antimicrobial activities assessment of fabricated selenium nanoparticles using *Pelargonium zonale* leaf extract. *Green Process Synth.* 2019;8(1):191–8. <https://doi.org/10.1515/gps-2018-0060>
42. Menon S, KS SD, Agarwal H, Shanmugam VK. Efficacy of biogenic selenium nanoparticles from an extract of ginger towards evaluation on anti-microbial and anti-oxidant activities. *Colloid Interface Sci Commun.* 2019;29:1–8. <https://doi.org/10.1016/j.colcom.2018.12.004>